

Frozen light in periodic metamaterials

Alex Figotin and Ilya Vitebskiy

Abstract. Wave propagation in spatially periodic media, such as photonic crystals, can be qualitatively different from any uniform substance. The differences are particularly pronounced when the electromagnetic wavelength is comparable to the primitive translation of the periodic structure. In such a case, the periodic medium cannot be assigned any meaningful refractive index. Still, such features as negative refraction and/or opposite phase and group velocities for certain directions of light propagation can be found in almost any photonic crystal. The only reservation is that unlike hypothetical uniform left-handed media, photonic crystals are essentially anisotropic at frequency range of interest. Consider now a plane wave incident on a semi-infinite photonic crystal. One can assume, for instance, that in the case of positive refraction, the normal components of the group and the phase velocities of the transmitted Bloch wave have the same sign, while in the case of negative refraction, those components have opposite signs. What happens if the normal component of the transmitted wave group velocity vanishes? Let us call it a "zero-refraction" case. At first sight, zero normal component of the transmitted wave group velocity implies total reflection of the incident wave. But we demonstrate that total reflection is not the only possibility. Instead, the transmitted wave can appear in the form of an abnormal grazing mode with huge amplitude and nearly tangential group velocity. This spectacular phenomenon is extremely sensitive to the frequency and direction of propagation of the incident plane wave. These features can be very attractive in numerous applications, such as higher harmonic generation and wave mixing, light amplification and lasing, highly efficient superprisms, etc.

1. Introduction

Wave propagation in spatially periodic media, such as photonic crystals, is qualitatively different from that of any uniform substance. The differences are particularly pronounced when the wavelength is comparable to the primitive translation L of the periodic structure [1, 2, 3, 4, 5, 6, 7]. The effects of strong spatial dispersion culminate when the group velocity of a traveling Bloch wave vanishes. One reason for this is that vanishing group velocity always implies a dramatic increase in density of modes at the respective frequency. In addition, vanishing group velocity also implies certain qualitative changes in the eigenmode structure, which can be accompanied by some spectacular effects in electromagnetic wave propagation. A particular example of the kind is the frozen mode regime associated with a dramatic enhancement of the wave transmitted to the periodic medium [8, 9, 10, 11, 12, 13]. In this paper we consider several different modifications of the frozen mode regime, each related to a specific singularity of the electromagnetic dispersion relation. For every case we present specific examples of periodic dielectric structures supporting such a phenomenon. For the most part, we restrict ourselves to periodic layered media, which are photonic crystals with one dimensional periodicity.

We start with the simple case of a plane electromagnetic wave normally incident on a semi-infinite periodic layered structure. In the case of normal incidence, there are two different kinds of frozen mode regime. The first one is associated with a stationary inflection point of the dispersion relation in Fig. 1(b). In this case the incident plane wave of frequency ω_0 is converted into the frozen mode with infinitesimal group velocity and very large diverging amplitude. A detailed description of this phenomenon can be found in our previous publications on this subject [8, 9, 10, 11, 12, 13]. Qualitatively different kind of frozen mode regime occurs in the vicinity of a degenerate photonic band edge, shown in Fig. 1(c). In this latter case, the incident wave of frequency ω_d is reflected back to space, but not before it creates a frozen mode with huge diverging amplitude. Not every periodic structure can support the frozen mode regime. Specifically, in the case of a normal incident, a unit cell of the periodic layered array must contain at least three layers, of which two must display a misaligned in-plane anisotropy, as shown in Fig. 2. In photonic crystals with three dimensional periodicity, the presence of anisotropic constitutive component is not necessary.

In Section 3, we turn to the case of oblique wave propagation, which is of particular interest here. The frozen mode regime at oblique incidence can occur when the normal component of the transmitted wave group velocity vanishes, while its tangential component remains finite. In such a case, the transmitted wave is an abnormal grazing mode with a dramatically enhanced amplitude and nearly tangential energy flux. Remarkably, the photonic crystal reflectivity at this point can be very low, implying almost total conversion of the incident plane wave into the abnormal grazing mode. A significant advantage of this phenomenon is that it can occur in much simpler periodic structures, compared to those supporting the frozen mode regime at normal incidence. Examples are shown in Fig. 3 and 4. The presence of anisotropic layers is still required.

Yet another interesting modification of the frozen mode regime is an abnormal subsurface wave in the vicinity of a degenerate photonic band edge. A regular surface wave usually decays exponentially with the distance from the surface in either direction. By contrast, the abnormal subsurface wave is extremely asymmetric. It does decay rapidly outside the photonic crystal. But inside the periodic medium, its

amplitude sharply increases, and reaches its maximum at a certain distance from the surface. Only after that the field amplitude begins a slow decay, as the distance from the surface further increases. The profile of such a subsurface wave is similar to that of the frozen mode in the vicinity of a degenerate band edge. This phenomenon is briefly discussed in section 4.

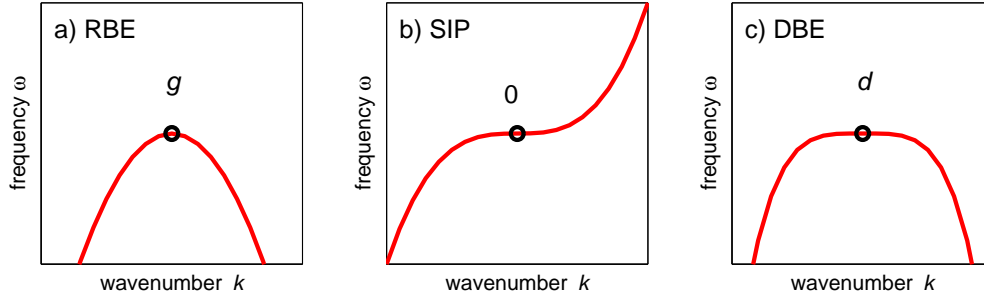


Figure 1. Fragments of dispersion relations containing different stationary points: (a) a regular band edge (RBE) g , (b) a stationary inflection point (SIP) 0 , (c) a degenerate band edge (DBE) d .

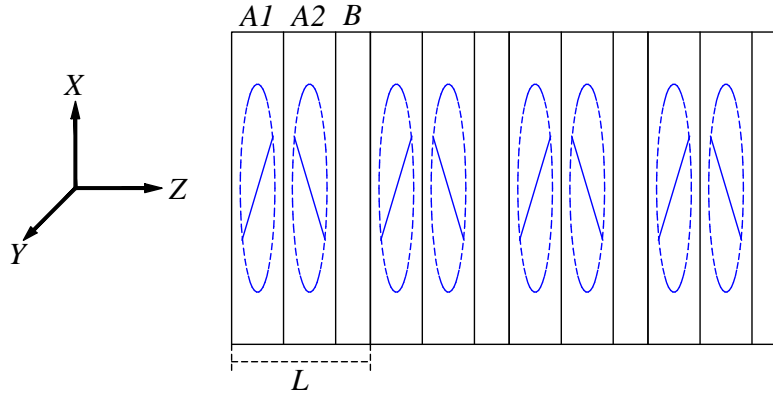


Figure 2. Periodic stack capable of supporting $k - \omega$ diagram with degenerate band edge. A unit cell L includes three layers: two birefringent layers A_1 and A_2 with misaligned in-plane anisotropy and one isotropic B layer. The misalignment angle $\varphi = \varphi_1 - \varphi_2$ between adjacent anisotropic layers A_1 and A_2 must be different from 0 and $\pi/2$.

2. Frozen mode regime at normal incidence

The essence of the frozen mode regime can be understood from the example of a plane monochromatic wave normally incident on a semi-infinite periodic layered structure, as shown in Fig. 5. An important requirement, though, is that some of the layers

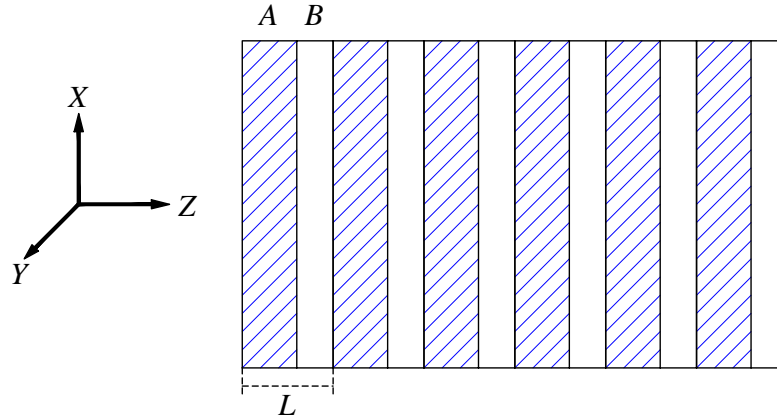


Figure 3. Periodic layered structure with two layers A and B in a primitive cell L . The A layers (hatched) are anisotropic with one of the principle axes of the dielectric permittivity tensor making an oblique angle with the normal z to the layers ($\epsilon_{xz} \neq 0$). The B layers are isotropic. The $x - z$ plane coincides with the mirror plane of the stack.

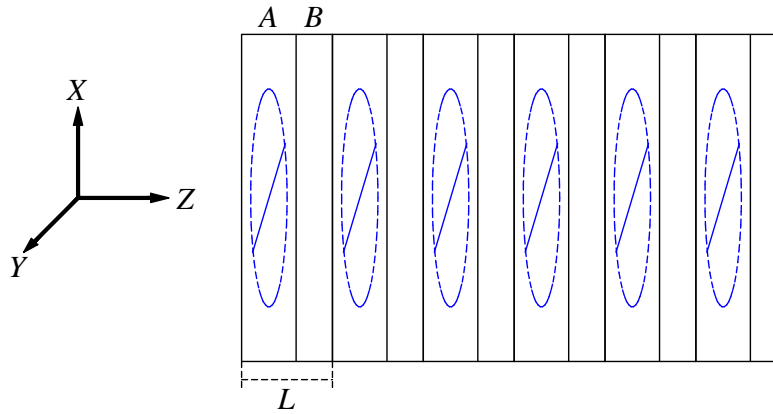


Figure 4. Periodic layered structure with two layers A and B in a unit cell L . The A layer has inplane anisotropy, while the B layer can be isotropic.

must display a misaligned in-plane anisotropy. The simplest periodic layered array of the kind is shown in Fig. 2.

To start with, let us introduce some basic notations and definitions. Let Ψ_I , Ψ_R , and Ψ_T be the incident, reflected and transmitted waves, respectively. Assume for now that all three monochromatic waves propagate along the z axis normal to the boundary of semi-infinite periodic layered structure in Figs. 5. The photonic crystal boundary is located at $z = 0$. Electromagnetic field both inside (at $z > 0$) and outside (at $z < 0$) the periodic stack is independent of the x and y coordinates, and

its transverse components can be represented as a column-vector

$$\Psi(z) = \begin{bmatrix} E_x(z) \\ E_y(z) \\ H_x(z) \\ H_y(z) \end{bmatrix}, \quad (1)$$

where $\vec{E}(z)$ and $\vec{H}(z)$ are time-harmonic electric and magnetic fields. We also assume that anisotropic layers of the periodic array have in-plane anisotropy, so the fields $\vec{E}(z)$ and $\vec{H}(z)$ are normal to the direction of propagation

$$\vec{E}(z) \perp z, \vec{H}(z) \perp z. \quad (2)$$

All four transverse field components in (1) are continuous functions of z , which leads to the following standard boundary condition at $z = 0$

$$\Psi_T(0) = \Psi_I(0) + \Psi_R(0). \quad (3)$$

Note that the polarizations of the incident, reflected and transmitted waves can be different, because some of the layers of the periodic array display an in-plane anisotropy, as shown in the example in Fig. 2. The latter is essential for the possibility of the frozen mode regime.

In periodic layered media, the electromagnetic eigenmodes $\Psi_k(z)$ are usually chosen in the Bloch form

$$\Psi_k(z + L) = e^{ikL} \Psi_k(z), \quad (4)$$

where the Bloch wavenumber k is defined up to a multiple of $2\pi/L$. The correspondence between ω and k is referred to as the Bloch dispersion relation. Real k correspond to propagating (traveling) Bloch modes. Propagating modes belong to different spectral branches $\omega(k)$ separated by frequency gaps. The speed of a traveling wave in periodic medium is determined by the group velocity [4]

$$u = d\omega/dk. \quad (5)$$

Normally, each spectral branch $\omega(k)$ develops stationary points $\omega_s = \omega(k_s)$ where the group velocity (5) of the corresponding propagating mode vanishes

$$d\omega/dk = 0, \text{ at } \omega = \omega_s = \omega(k_s). \quad (6)$$

Examples of different stationary points are shown in Fig. 1, where each of the frequencies ω_g , ω_0 and ω_d is associated with zero group velocity of the respective traveling wave. Stationary points (5) play essential role in the formation of frozen mode regime.

By contrast, evanescent Bloch modes are characterized by complex wavenumbers $k = k' + ik''$. Evanescent modes decay exponentially with the distance z from the boundary of semi-infinite periodic structure. Therefore, under normal circumstances, evanescent contribution to the transmitted wave $\Psi_T(z)$ can be significant only in close proximity of the surface. The situation can change dramatically when the frequency ω approaches one of the stationary point values ω_s . At first sight, stationary points (6) relate only to propagating Bloch modes. But in fact, in the vicinity of every stationary point frequency ω_s , the imaginary part k'' of the Bloch wavenumber of at least one of

the evanescent modes also vanishes. As a consequence, the respective evanescent mode decays very slowly, and its role may extend far beyond the photonic crystal boundary. In addition, in the special cases of interest, the electromagnetic field distribution $\Psi(z)$ in the coexisting evanescent and propagating eigenmodes becomes very similar, as ω approaches ω_s . This can result in spectacular resonance effects, such as the frozen mode regime. What exactly happens in the vicinity of a particular stationary point (6) essentially depends on its character and appears to be very different in each of the three cases presented in Fig. 1. In the next subsection we present a simple qualitative picture of the frozen mode regime based on energy conservation consideration. Then, in the following subsection, we provide more consistent analysis of the phenomenon.

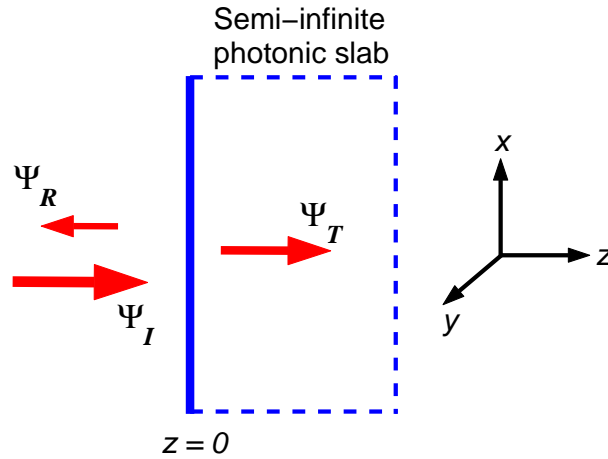


Figure 5. Plane wave normally incident on a semi-infinite photonic crystal. The subscripts I , R , and T refer to the incident, reflected and transmitted waves, respectively. In all cases, the amplitude of the incident wave is unity.

2.1. Energy density and energy flux at frozen mode regime

Let S_I , S_R and S_T be the energy flux in the incident, reflected and transmitted waves in Fig. 5. The transmission and reflection coefficients of a lossless semi-infinite medium are defined as

$$\tau = \frac{S_T}{S_I}, \quad \rho = -\frac{S_R}{S_I}, \quad (7)$$

where

$$S_I + S_R = S_T, \quad \rho = 1 - \tau.$$

With certain reservations, the energy flux S_T of the transmitted travelling wave can be expressed as

$$S_T = W_T u, \quad (8)$$

where u is the group velocity, which is also the energy velocity, and W_T is the energy density

$$W_T \propto |\Psi_T|^2.$$

Evanescent modes do not contribute to the normal energy flux S_T in the case of a lossless semi-infinite periodic structure. Besides, evanescent contribution to the transmitted wave becomes negligible at a certain distance z from the surface. The simple expression (8) may not apply when the transmitted wave involves two or more propagating Bloch modes, but we will not deal with such a situation here.

Vanishing group velocity u in (8) implies that the transmitted wave energy flux S_T also vanishes, along with the respective transmission coefficient τ in (7). The only exception could be if the energy density W_T of the transmitted wave increases dramatically in the vicinity of stationary point frequency. In other words, if W_T in (8) grows fast enough, as ω approaches ω_s , the product $W_T u$ in (8) can remain finite even at $\omega = \omega_s$. In such a case, a significant fraction of the incident radiation can be converted into the slow mode inside the semi-infinite periodic array. Hereinafter, the effect of a dramatic growth of the transmitted wave amplitude in the vicinity of a stationary point (6) will be referred to as the frozen mode regime. The possibility of such an effect is directly related to the character of a particular stationary point. From this point of view, let us consider three different situation presented in Fig. 1.

2.1.1. Regular band edge We start with the simplest case of a regular photonic band edge (RBE) shown in Fig. 1(a). It can be found in any periodic array, including any periodic layered structure. Just below the band edge frequency ω_g , the dispersion relation can be approximated by a quadratic parabola

$$\omega_g - \omega \propto (k - k_g)^2, \text{ at } \omega \lesssim \omega_g. \quad (9)$$

This yields the following frequency dependence of the propagating mode group velocity u below the photonic band edge

$$u = \frac{d\omega}{dk} \propto (k_g - k) \propto (\omega_g - \omega)^{1/2}, \text{ at } \omega \lesssim \omega_g. \quad (10)$$

Due to the boundary condition (3), the amplitude of the transmitted propagating Bloch mode in this case remains finite and comparable to that of the incident wave. Therefore, the energy flux (8) associated with the transmitted slow mode vanishes, as ω approaches ω_g

$$S_T = W_T u \propto \begin{cases} (\omega_g - \omega)^{1/2}, & \text{at } \omega \lesssim \omega_g \\ 0, & \text{at } \omega \geq \omega_g \end{cases}. \quad (11)$$

Formula (11) expresses the well-known fact that in the vicinity of a regular band edge, a lossless semi-infinite photonic crystal becomes totally reflective.

2.1.2. Stationary inflection point A completely different situation occurs in the vicinity of a stationary inflection point (SIP) shown in Fig. 1(b). Such a point can be found in periodic layered structures involving anisotropic and magnetic layers [8, 9], as well as in some photonic crystals with 2- and 3-dimensional periodicity. In the vicinity of a stationary inflection point ω_0 , the dispersion relation can be approximated by a cubic parabola

$$\omega - \omega_0 \propto (k - k_0)^3. \quad (12)$$

The propagating mode group velocity u vanishes as ω approaches ω_0 from either direction

$$u = \frac{d\omega}{dk} \propto (k - k_0)^2 \propto (\omega - \omega_0)^{2/3}. \quad (13)$$

But remarkably, the amplitude of the transmitted propagating mode increases so that the respective energy density W_T diverges as $\omega \rightarrow \omega_0$

$$W_T \propto (\omega - \omega_0)^{-2/3}. \quad (14)$$

The expression (13) together with (14) yield that the energy flux of the transmitted slow mode remains finite even at $\omega = \omega_0$

$$S_T = W_T u \sim S_I, \text{ at } \omega \approx \omega_0. \quad (15)$$

The latter implies that the incident light is converted to the frozen mode with infinitesimal group velocity (13) and huge diverging amplitude (14). Of course, in reality, the amplitude of the frozen mode will be limited by such factors as absorption, nonlinear effects, imperfection of the periodic dielectric array, deviation of the incident radiation from a perfect plane monochromatic wave, finiteness of the photonic crystal dimensions, etc. Still, with all these limitations in place, the frozen mode regime can be very attractive for a variety of practical applications.

2.1.3. Degenerate band edge Let us turn to the case of a degenerate band edge (DBE) shown in Fig. 1(c). Such a point can be found in dispersion relation of periodic layered structures involving misaligned anisotropic layers. An example is shown in Fig. 2. Just below the degenerate band edge frequency ω_d , the dispersion relation $\omega(k)$ can be approximated as

$$\omega_d - \omega \propto (k - k_d)^4, \text{ at } \omega \lesssim \omega_d \quad (16)$$

This yields the following frequency dependence of the propagating mode group velocity

$$u = \frac{d\omega}{dk} \propto (k_d - k)^3 \propto (\omega_d - \omega)^{3/4}, \text{ at } \omega \lesssim \omega_d. \quad (17)$$

The amplitude of the transmitted slow mode in this case diverges, as the frequency approaches the band edge value

$$W_T \propto |\omega_d - \omega|^{-1/2}, \text{ at } \omega \lesssim \omega_{DBE}, \quad (18)$$

which constitutes the frozen mode regime. But the amplitude does not grow fast enough to offset the vanishing group velocity (17). Indeed, the expressions (17) and (18) together with (8) yield for the energy flux

$$S_T = W_T u \propto \begin{cases} (\omega_d - \omega)^{1/4}, & \text{at } \omega \lesssim \omega_d \\ 0, & \text{at } \omega \geq \omega_d \end{cases}, \quad (19)$$

implying that, in spite of the diverging energy density (18), the energy flux of the transmitted slow wave vanishes, as ω approaches ω_d .

The situation at a degenerate band edge (16) can be viewed as intermediate between the frozen mode regime at a stationary inflection point (12), and the vicinity of a regular band edge (9). Indeed, on the one hand, the incident wave at $\omega = \omega_d$ is totally reflected back to space, as is the case at a regular band edge. On the other hand, the transmitted field amplitude inside the periodic medium becomes very large as $\omega \rightarrow \omega_d$, which is similar to what occurs at a stationary inflection point. The very large amplitude (18) of the transmitted wave at $\omega \approx \omega_d$ still can be very attractive for applications.

The above consideration does not explain the nature of the frozen mode regime, nor does it address the problem of the eigenmode composition of the frozen mode. All these questions are the subject of the next subsection.

2.2. Physical nature of the frozen mode regime

2.2.1. Eigenmode composition of transmitted wave In a periodic layered structure, at any given frequency ω , there are four electromagnetic eigenmodes with different polarizations and wavenumbers. But in the setting of Fig. 5 where the semi-infinite periodic layered array occupies the half-space $z \geq 0$, the transmitted wave is a superposition of only two of the four Bloch eigenmodes. Indeed, the propagating waves with negative group velocity do not contribute to $\Psi_T(z)$, nor do the evanescent modes exponentially growing with the distance z . Generally, one can distinguish three different possibilities.

- (i) Both Bloch components of the transmitted wave Ψ_T are propagating modes

$$\Psi_T(z) = \Psi_{pr1}(z) + \Psi_{pr2}(z), \quad z \geq 0. \quad (20)$$

The transmitted wave Ψ_T in (20) is composed of two Bloch eigenmodes with two different real wavenumbers k_1 and k_2 and two different group velocities $u_1 > 0$ and $u_2 > 0$. This constitutes the phenomenon of double refraction, provided that u_1 and u_2 are different. The other two Bloch components of the same frequency have negative group velocities and cannot contribute to the transmitted wave Ψ_T .

- (ii) Both Bloch components of Ψ_T are evanescent

$$\Psi_T(z) = \Psi_{ev1}(z) + \Psi_{ev2}(z), \quad z \geq 0. \quad (21)$$

The respective two values of k are complex with positive imaginary parts $k'' > 0$. This is the case when the frequency ω falls into photonic band gap at $\omega > \omega_g$ in Fig. 1(a) or at $\omega > \omega_d$ in Fig. 1(c). The fact that $k'' > 0$ implies that the wave amplitude decays with the distance z from the surface of the semi-infinite photonic crystal. In the case (21), the incident wave is totally reflected back to space by the semi-infinite periodic structure.

- (iii) One of the Bloch components of the transmitted wave Ψ_T is a propagating mode with $u > 0$, while the other is an evanescent mode with $k'' > 0$

$$\Psi_T(z) = \Psi_{pr}(z) + \Psi_{ev}(z), \quad z \geq 0. \quad (22)$$

For example, this is the case at $\omega \sim \omega_0$ in Fig. 1(b), as well as at $\omega < \omega_g$ in Fig. 1(a) and at $\omega < \omega_d$ in Fig. 1(c). As the distance z from the surface increases, the evanescent contribution Ψ_{ev} in (22) decays as $\exp(-zk'')$, and the resulting transmitted wave $\Psi_T(z)$ turns into a single propagating Bloch mode Ψ_{pr} .

Propagating modes with $u < 0$, as well as evanescent modes with $k'' < 0$, never contribute to the transmitted wave Ψ_T inside the semi-infinite stack in Fig. 5. This statement is based on the following two assumptions:

- The transmitted wave Ψ_T and the reflected wave Ψ_R are originated from the plane wave Ψ_I incident on the semi-infinite photonic slab from the left, as shown in Fig. 5.
- The layered array in Fig. 5 occupies the entire half-space and is perfectly periodic at $z > 0$.

If either of the above conditions is violated, the electromagnetic field inside the periodic stack can be a superposition of four Bloch eigenmodes with either sign of the group velocity u of propagating contributions, or either sign of k'' of evanescent contributions. For example, this would be the case if the periodic layered array in Fig. 5 had some kind of structural defects or a finite thickness.

The propagating modes with $u > 0$ and evanescent modes with $k'' > 0$ are referred to as *forward* waves. Only forward modes contribute to the transmitted wave $\Psi_T(z)$ in the case of a periodic semi-infinite stack. The propagating modes with $u < 0$ and evanescent modes with $k'' < 0$ are referred to as *backward* waves. Since the backward Bloch waves are not excited in the setting of Fig. 5, they play no role in further consideration.

Note that the assumption that the transmitted wave $\Psi_T(z)$ is a superposition of propagating and/or evanescent Bloch eigenmodes may not apply if the frequency ω exactly coincides with one of the stationary point frequencies (6). For example, at frequency ω_0 of stationary inflection point, there are no evanescent eigenmodes at all, and the transmitted wave $\Psi_T(z)$ is a (non-Bloch) Floquet eigenmode linearly growing with z [9]. The term non-Bloch means that the respective field distribution does not comply with the relation (4). Similar situation occurs at frequency ω_d of degenerate band edge. At the same time, at any general frequency, including the vicinity of any stationary point (6), the transmitted wave $\Psi_T(z)$ is a superposition of two Bloch eigenmodes, each of which is either propagating, or evanescent.

In all three cases (20 – 22), the contribution of a particular Bloch eigenmode to the transmitted wave Ψ_T depends on the polarization Ψ_I of the incident wave. One can always choose some special incident wave polarization, such that only one of the two forward Bloch modes is excited and the transmitted wave Ψ_T is a single Bloch eigenmode. In the next subsection we will see that there is no frozen mode regime in the case of a single mode excitation. This fact relates to the very nature of the frozen mode regime.

Knowing the eigenmode composition of the transmitted wave we can give a semi-qualitative description of what happens when the frequency ω of the incident wave approaches one of the stationary points (6) in Fig. 1. A consistent mathematical analysis of the asymptotic behavior in the vicinity of different stationary points is rather complicated. The details can be found in [13] and references therein.

2.2.2. Regular photonic band edge We start with the simplest case of a regular photonic band edge. There are two different possibilities in this case, but none of them is associated with the frozen mode regime. The first one relates to the trivial case where none of the layers of the periodic structure displays an in-plane anisotropy or gyrotropy. As the result, all Bloch eigenmodes are doubly degenerate with respect to polarization. A detailed description of this case can be found in textbooks on optics. Slightly different scenario occurs if some of the layers are anisotropic or gyrotropic and, as a result, the polarization degeneracy is lifted. Just below the band edge frequency ω_g in Fig. 1(a), the transmitted field $\Psi_T(z)$ is a superposition (22) of one propagating and one evanescent Bloch modes. Due to the boundary condition (3), the amplitude of the transmitted wave at $z = 0$ is comparable to that of the incident wave. In the case of a generic polarization of the incident light, the amplitudes of the propagating and evanescent Bloch components at $z = 0$ are also comparable to each other and to

the amplitude of the incident light

$$|\Psi_{pr}(0)| \sim |\Psi_{ev}(0)| \sim |\Psi_I|, \text{ at } \omega \leq \omega_g. \quad (23)$$

As the distance z from the surface increases, the evanescent component $\Psi_{ev}(z)$ decays rapidly, while the amplitude of the propagating component remains constant. Eventually, at a certain distance from the slab surface, the transmitted wave $\Psi_T(z)$ becomes very close to the propagating mode

$$\Psi_T(z) \approx \Psi_{pr}(z), \text{ at } z \gg L, \omega \leq \omega_g. \quad (24)$$

The evanescent component Ψ_{ev} of the transmitted wave does not display any singularity at the band edge frequency ω_g . The propagating mode Ψ_{pr} does develop a singularity associated with vanishing group velocity at $\omega \rightarrow \omega_g - 0$, but its amplitude remains finite and comparable to that of the incident wave. At $\omega > \omega_g$, this propagating mode turns into another evanescent mode in (21). The bottom line is that none of the Bloch components of the transmitted wave develops a large amplitude in the vicinity of a regular photonic band edge. There is no frozen mode regime in this case.

2.2.3. Stationary inflection point A completely different situation develops in the vicinity of a stationary inflection point (12) of the dispersion relation. At $\omega \approx \omega_0$, the transmitted wave Ψ_T is a superposition (22) of one propagating and one evanescent Bloch component. In contrast to the case of a regular photonic band edge, in the vicinity of ω_0 both Bloch contributions to Ψ_T develop strong singularity. Specifically, as the frequency ω approaches ω_0 , both contributions grow dramatically, while remaining nearly equal and opposite in sign at the slab boundary [9]

$$\Psi_{pr}(0) \approx -\Psi_{ev}(0) \propto |\omega - \omega_0|^{-1/3}, \text{ as } \omega \rightarrow \omega_0. \quad (25)$$

Due to the destructive interference (25), the resulting field

$$\Psi_T(0) = \Psi_{pr}(0) + \Psi_{ev}(0)$$

at the photonic crystal surface is small enough to satisfy the boundary condition (3), as illustrated in Figs. 6 and 7. As the distance z from the slab boundary increases, the destructive interference becomes less effective – in part because the evanescent contribution decays exponentially

$$\Psi_{ev}(z) \approx \Psi_{ev}(0) \exp(-zk'') \quad (26)$$

while the amplitude of the propagating contribution remains constant and very large. Eventually, the transmitted wave $\Psi_T(z)$ reaches its large saturation value corresponding to its propagating component Ψ_{pr} , as illustrated in Fig. 7.

Note that the imaginary part k'' of the evanescent mode wavenumber in (26) also vanishes in the vicinity of stationary inflection point

$$k'' \propto |\omega - \omega_0|^{1/3}, \text{ as } \omega \rightarrow \omega_0, \quad (27)$$

reducing the rate of decay of the evanescent contribution (26). As a consequence, the resulting amplitude $\Psi_T(z)$ of the transmitted wave reaches its large saturation

value Ψ_{pr} only at a certain distance Z from the surface. This characteristic distance increases as the frequency approaches its critical value ω_0

$$Z \propto 1/k'' \propto |\omega - \omega_0|^{-1/3}. \quad (28)$$

If the frequency of the incident wave is exactly equal to the frozen mode frequency ω_0 , the transmitted wave $\Psi_T(z)$ does not reduce to the sum (22) of propagating and evanescent contributions, because at $\omega = \omega_0$ there is no evanescent solutions to the Maxwell equations. Instead, $\Psi_T(z)$ corresponds to a non-Bloch Floquet eigenmode diverging linearly with z [9]

$$\Psi_T(z) - \Psi_T(0) \propto z\Psi_0, \quad \text{at } \omega = \omega_0. \quad (29)$$

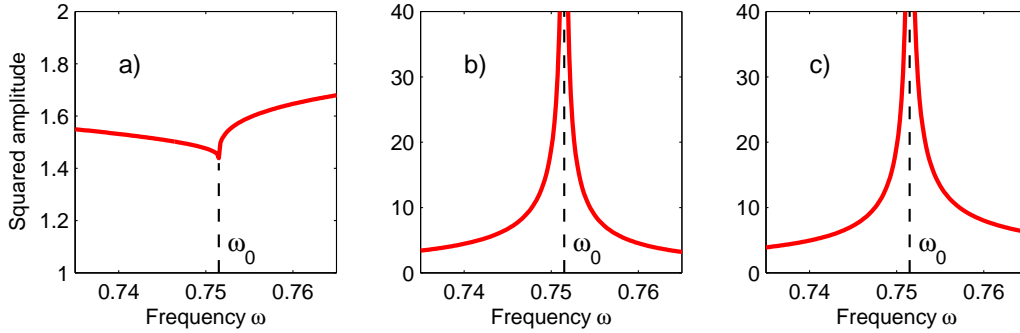


Figure 6. Frequency dependence of squared amplitude of the transmitted wave (a), as well as its propagating (b) and evanescent (c) components at the surface of semi-infinite photonic crystal at $z = 0$. The stationary inflection point frequency is ω_0 . Due to the destructive interference (25) of the propagating and evanescent contributions, the amplitude (a) of the resulting transmitted field remains small enough to satisfy the boundary conditions. The amplitude of the incident wave is unity.

2.2.4. Degenerate band edge While the situation with a regular photonic band edge (9) appears trivial, the case of a degenerate band edge (16) proves to be quite different. Below the degenerate band edge frequency ω_d , the transmitted field is a superposition (22) of one propagating and one evanescent components, while above ω_d , the transmitted wave is a combination (21) of two evanescent components. In this respect, the regular and degenerate band edges are similar to each other. A crucial difference, though, is that in the vicinity of a degenerate band edge, both Bloch contributions to the transmitted wave diverge as ω approaches ω_d , which constitutes the frozen mode regime.

Let us start with the transmission band at $\omega < \omega_d$. As the frequency ω approaches $\omega_d - 0$, both Bloch contributions in (22) grow sharply, while remaining nearly equal and opposite in sign at the surface

$$\Psi_{pr}(0) \approx -\Psi_{ev}(0) \propto |\omega_d - \omega|^{-1/4}, \quad \text{as } \omega \rightarrow \omega_d - 0. \quad (30)$$

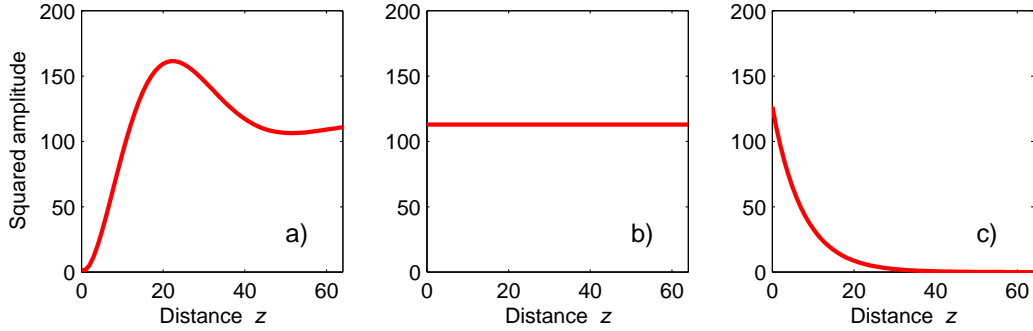


Figure 7. Destructive interference of the propagating and evanescent components of the transmitted wave inside semi-infinite photonic crystal at $z > 0$. The frequency is close but not equal to that of the stationary inflection point. (a) The squared amplitude $|\Psi_T(z)|^2$ of the resulting transmitted field – its amplitude at $z = 0$ is small enough to satisfy the boundary conditions; (b) the squared amplitude $|\Psi_{pr}(z)|^2$ of the propagating contribution; (c) the squared amplitude $|\Psi_{ev}(z)|^2$ of the evanescent contribution. The amplitude of the incident wave is unity. The distance z from the surface is expressed in units of L .

The destructive interference (30) ensures that the boundary condition (3) can be satisfied, while both Bloch contributions to $\Psi_T(z)$ diverge. As the distance z from the slab boundary increases, the evanescent component $\Psi_{ev}(z)$ dies out

$$\Psi_{ev}(z) \approx \Psi_{ev}(0) \exp(-zk'') \quad (31)$$

while the propagating component $\Psi_{pr}(z)$ remains very large. Eventually, as the distance z further increases, the transmitted wave $\Psi_T(z)$ reaches its large saturation value corresponding to its propagating component $\Psi_{pr}(z)$, as illustrated in Fig. 8. Note that the imaginary part k'' of the evanescent mode wavenumber also vanishes in the vicinity of degenerate band edge

$$k'' \propto |\omega - \omega_d|^{1/4}, \text{ as } \omega \rightarrow \omega_d, \quad (32)$$

reducing the rate of decay of the evanescent contribution (31). As a consequence, the resulting amplitude $\Psi_T(z)$ of the transmitted wave reaches its large saturation value Ψ_{pr} only at a certain distance Z from the surface. This characteristic distance increases as the frequency approaches its critical value ω_d

$$Z \propto 1/k'' \propto |\omega - \omega_d|^{-1/4}, \quad (33)$$

as illustrated in Fig. 10(a, b). If the frequency ω of the incident wave is exactly equal to ω_d , the transmitted wave $\Psi_T(z)$ does not reduce to the sum of two Bloch contributions. Instead, it corresponds to a non-Bloch Floquet eigenmode linearly diverging with z

$$\Psi_T(z) - \Psi_T(0) \propto z\Psi_d, \text{ at } \omega = \omega_d. \quad (34)$$

This situation is illustrated in Fig. 10(c).

The above behavior appears to be very similar to that of the frozen mode regime at a stationary inflection point, shown in Fig. 7. Yet, there is a crucial difference between

the two cases. Indeed, according to (19), in the immediate proximity of a degenerate band edge, the Poynting vector S_T of the transmitted wave Ψ_T is infinitesimal, in spite of the diverging wave amplitude (30). In other words, although the energy density $W_T \propto |\Psi_T|^2$ of the frozen mode diverges as $\omega \rightarrow \omega_d - 0$, it does not grow fast enough to offset the vanishing group velocity (17). As a consequence, the photonic crystal becomes totally reflective at $\omega = \omega_d$. Of course, the total reflectivity persists at $\omega > \omega_d$, where there is no propagating modes at all. By contrast, in the case (29) of a stationary inflection point, the respective Poynting vector S_T is finite and can be even close to that of the incident wave. The latter implies low reflectivity and nearly total conversion of the incident wave energy into the frozen mode.

Interesting situation occurs when we approach the degenerate band edge frequency from the band gap. In such a case, the transmitted field $\Psi_T(z)$ is a superposition (21) of two evanescent components. As the frequency ω approaches ω_d . Both evanescent contributions grow sharply, while remaining nearly equal and opposite in sign at the photonic crystal boundary

$$\Psi_{ev1}(0) \approx -\Psi_{ev2}(0) \propto |\omega_d - \omega|^{-1/4}, \quad \text{as } \omega \rightarrow \omega_d + 0. \quad (35)$$

Again, the destructive interference (35) ensures that the boundary condition (3) is satisfied, while both evanescent contributions to $\Psi_T(z)$ diverge in accordance with (35). As the distance z from the slab boundary increases, the destructive interference of these two evanescent components is lifted and the resulting field amplitude increases sharply, as shown in Fig. 9. But eventually, as the distance z further increases, the transmitted wave $\Psi_T(z)$ completely decays, because both Bloch contributions to $\Psi_T(z)$ are evanescent. The latter constitutes the major difference between the frozen mode regime above and below the DBE frequency ω_d . The rate of the amplitude decay, as well as the position of the maximum of the transmitted wave amplitude in Fig. 9(a), are determined by the characteristic distance Z in (33).

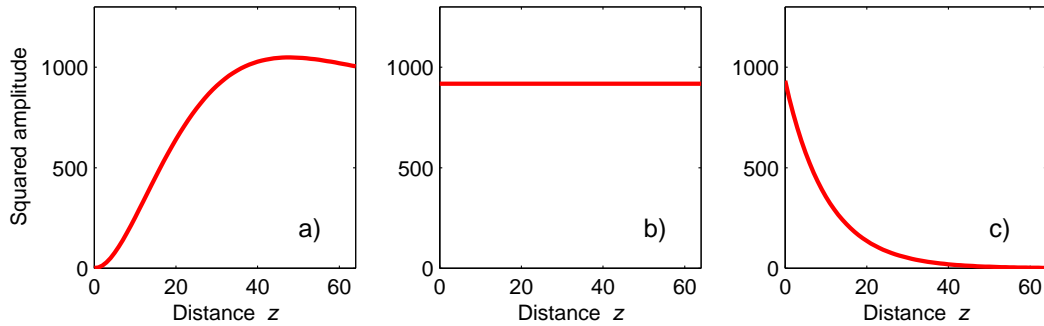


Figure 8. Smoothed field distribution in the transmitted wave (a), along with its propagating (b) and evanescent (c) components at frequency slightly below that of the degenerate band edge in Fig. 1(c). The amplitude of the incident wave is unity. Similar graphs related to the stationary inflection point in Fig. 1(b) are shown in Fig.6

2.2.5. Physical reason for the growing wave amplitude The wave $\Psi_T(z)$ transmitted to the semi-infinite periodic layered medium is a superposition of two forward Bloch

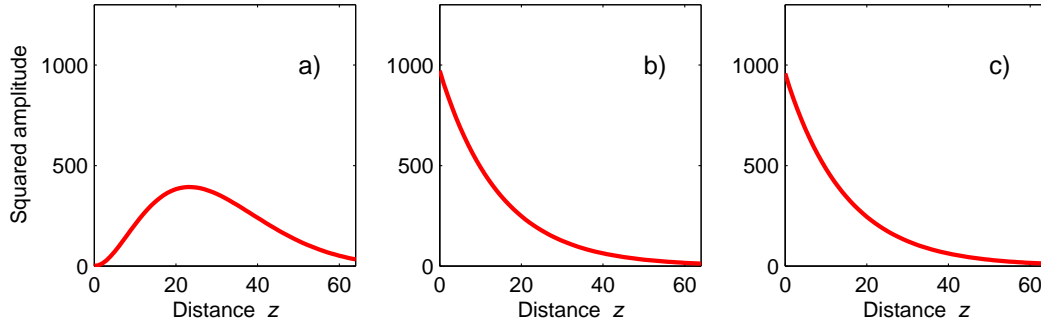


Figure 9. Smoothed field distribution in the transmitted wave (a), along with its two evanescent components (b) and (c), at a band gap frequency just above the degenerate band edge value ω_d in Fig. 1(c). Compare these graphs with those in Fig. 8, where the frequency lies in the transmission band below ω_d .

modes $\Psi_1(z)$ and $\Psi_2(z)$

$$\Psi_T(z) = \Psi_1(z) + \Psi_2(z). \quad (36)$$

The two eigenmodes in (36) can be a propagating and an evanescent, as in the case (22), or they can be both evanescent, as in the case (21). The physical reason for the sharp increase in the transmitted wave amplitude at the frozen mode regime is that the two Bloch eigenmodes contributing to $\Psi_T(z)$ become nearly indistinguishable from each other, as the frequency approaches its critical value

$$\Psi_1(z) \approx \alpha \Psi_2(z), \quad \text{as } \omega \rightarrow \omega_s, \quad (37)$$

where α is a scalar, and ω_s is the frozen mode frequency (ω_0 or ω_d).

Let us show under what circumstances the property (37) can lead to the frozen mode regime. The sum (36) of two nearly parallel column vectors Ψ_1 and Ψ_2 must match the boundary conditions (3) with the incident and reflected waves. If the incident wave polarization is general, then the nearly parallel Bloch components Ψ_1 and Ψ_2 must be very large and nearly equal and opposite

$$\Psi_1(0) \approx -\Psi_2(0), \quad |\Psi_1(0)| \approx |\Psi_2(0)| \gg |\Psi_I|, \quad (38)$$

in order to satisfy the boundary conditions (3). Indeed, since the incident field polarization is general, we have no reason to expect that the column vector $\Psi(0)$ at the surface is nearly parallel to $\Psi_1(0)$ and $\Psi_2(0)$. But on the other hand, the boundary conditions say that

$$\Psi(0) = \Psi_1(0) + \Psi_2(0) \quad (39)$$

Obviously, the only situation where the sum (39) of two nearly parallel vectors can be not nearly parallel to either of them is the one described in (38).

There is one exception, though. Recall that in the vicinity of the frozen mode frequency, the two Bloch components Ψ_1 and Ψ_2 of the transmitted wave are nearly parallel to each other (see formula (37)). For this reason, if the polarization of the incident wave is such that $\Psi(0)$ in (39) is nearly parallel to any of the Bloch eigenmodes

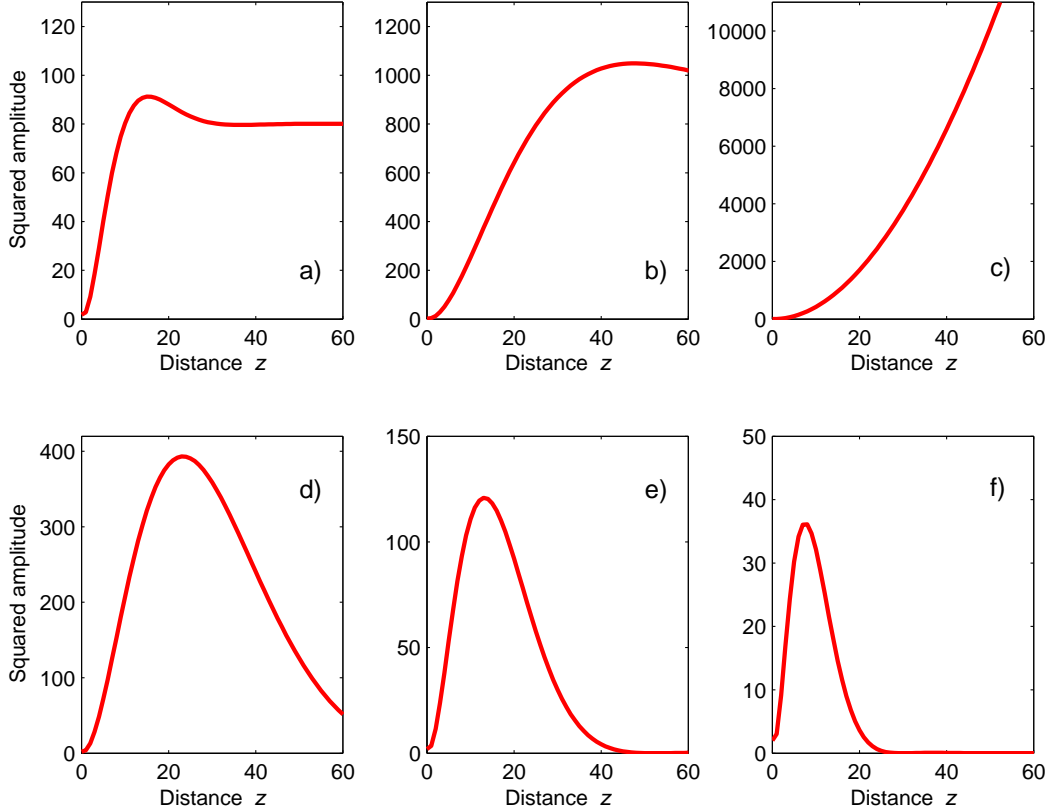


Figure 10. Smoothed profile of the frozen mode at six different frequencies in the vicinity of degenerate band edge: (a) $\omega = \omega_d - 10^{-4}c/L$, (b) $\omega = \omega_d - 10^{-6}c/L$, (c) $\omega = \omega_d$, (d) $\omega = \omega_d + 10^{-6}c/L$, (e) $\omega = \omega_d + 10^{-5}c/L$, (f) $\omega = \omega_d + 10^{-4}c/L$. In the transmission band at $\omega < \omega_d$, the asymptotic field value is very large and diverges as $\omega \rightarrow \omega_d$. By contrast, in the band gap at $\omega > \omega_d$, the asymptotic field value is zero. In all cases, the amplitude of the incident wave is unity.

$\Psi_1(0)$ and $\Psi_2(0)$, it is also nearly parallel to both of them. In this, and only this case, the amplitude of the transmitted wave $\Psi_T(z)$ will be comparable to that of the incident wave. There is no frozen mode regime for this narrow range of the incident wave polarization. A particular case of the above situation is a regime of a single mode excitation, where only one of the two Bloch components Ψ_1 or Ψ_2 in (36) contributes to the transmitted wave.

Finally, let us reiterate that in the limiting cases of $\omega = \omega_0$ or $\omega = \omega_d$, the transmitted wave $\Psi_T(z)$ corresponds to a non-Bloch Floquet eigenmode (29) or (34), respectively. Either of them linearly diverges with z . Again, the only exception is when the incident wave has the unique polarization, at which the transmitted wave $\Psi_T(z)$ is a propagating Bloch eigenmode with zero group velocity and a limited amplitude, comparable to that of the incident wave.

3. Oblique propagation. Abnormal grazing modes

A phenomenon similar to the frozen mode regime can also occur in the case of oblique wave propagation, where the incident, reflected and transmitted waves are all propagate at an angle to the z axis, as shown in Fig. 11. Consider the situation where the normal component u_z of the group velocity of the transmitted propagating wave vanishes, while the tangential component \vec{u}_\perp remains finite.

$$u_z = \frac{\partial\omega}{\partial k_z} = 0, \quad \vec{u}_\perp = \frac{\partial\omega}{\partial \vec{k}_\perp} \neq 0, \quad \text{at } \omega = \omega_s = \omega(\vec{k}_s) \quad (40)$$

This is exactly what happens in the vicinity of the well-known phenomenon of total internal reflection [6]. Similar phenomenon can be found in any photonic crystal at frequency corresponding to the transmission band edge for a particular direction of incidence. Remarkably, the total reflection of the incident wave is not the only possible outcome. Another alternative is that the transmitted wave forms an abnormal grazing mode with dramatically enhanced amplitude and tangential group velocity. The photonic crystal reflectivity at the critical point (40) can be even low – quite the opposite to what happens at total internal reflection. Low reflectivity implies that in spite of the vanishing normal component u_z of the transmitted wave group velocity, almost all the energy of the incident wave is converted into an abnormal grazing mode with drastically enhanced amplitude. The profile of such a grazing mode, i.e., the field dependence on the distance z from the surface, appears to be very similar to that of the frozen mode at normal incidence shown in Figs. 7, 8, 9, and 10. The only difference is that the tangential component of the group velocity at an oblique version of the frozen mode regime can be large and comparable to the speed of light in vacuum. A significant advantage of the oblique version of the frozen mode regime is that it can occur in much simpler periodic structures, compared to those supporting the frozen mode regime at normal incidence. Examples of periodic layered arrays supporting only the oblique version of the frozen mode regime are shown in Figs. 3 and 4. These structures are too simple to support any kind of frozen mode regime at normal incidence – they have only two different layers per unit cell, of which only one layer is anisotropic. But at oblique incidence, these relatively simple periodic arrays can support the frozen mode regime. The presence of at least one anisotropic layer in a unit cell L is still required.

Further in this section we outline some basic properties of the frozen mode regime at oblique incidence.

3.1. Axial dispersion relation: basic definitions

Consider a plane monochromatic wave obliquely incident on a periodic semi-infinite stack, as shown in Fig. 11. Due to the boundary conditions (3), the incident, reflected and transmitted waves should be assigned the same pair of tangential components k_x, k_y of the respective wave vectors

$$\left(\vec{k}_I\right)_x = \left(\vec{k}_R\right)_x = \left(\vec{k}_T\right)_x, \quad \left(\vec{k}_I\right)_y = \left(\vec{k}_R\right)_y = \left(\vec{k}_T\right)_y, \quad (41)$$

while the axial (normal) components k_z are all different. For the incident and reflected waves we have simply

$$\left(\vec{k}_I\right)_z = -\left(\vec{k}_R\right)_z = \sqrt{\omega^2 c^2 - k_x^2 - k_y^2}. \quad (42)$$

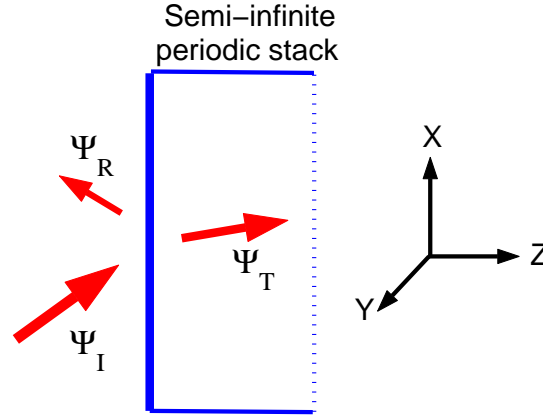


Figure 11. Scattering problem for a plane wave obliquely incident on a semi-infinite periodic layered medium. The arrows schematically shows the Pointing vectors of the incident, reflected and transmitted waves. The energy flux S_I of the incident plane wave is unity.

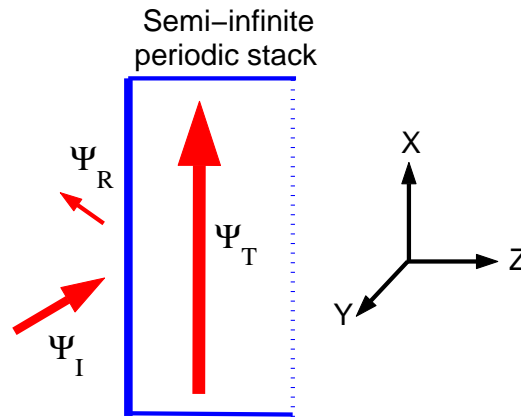


Figure 12. The case of oblique incidence, where the transmitted wave is a grazing mode with very large amplitude and purely tangential energy flux.

Let us turn to the transmitted wave. The transmitted wave is usually a composition of two Bloch eigenmodes with the same $\vec{k}_\perp = (k_x, k_y)$ from (41), but different k_z . For given \vec{k}_\perp and ω , the value of k_z is obtained by solving the time-harmonic Maxwell equations in the periodic medium. The so found correspondence between the wavenumber k_z and the frequency ω at fixed \vec{k}_\perp is referred to as the *axial* or *normal* dispersion relation. Real k_z correspond to propagating (traveling) Bloch modes, while complex k_z correspond to evanescent modes, decaying with the distance z from the surface. Unlike k_x and k_y , the Bloch wavenumber k_z is defined up to a multiple of $2\pi/L$.

Similarly to the case of normal propagation, the expression (40) defines stationary points of the axial dispersion relation. The definition (40) is a generalization of (6) to the case of oblique propagation. Different kinds of axial stationary points are defined

as follows.

- A regular band edge of axial dispersion relation

$$\frac{\partial\omega}{\partial k_z} = 0, \quad \frac{\partial^2\omega}{\partial k_z^2} \neq 0 \quad (43)$$

- A stationary inflection point of axial dispersion relation

$$\frac{\partial\omega}{\partial k_z} = 0, \quad \frac{\partial^2\omega}{\partial k_z^2} = 0, \quad \frac{\partial^3\omega}{\partial k_z^3} \neq 0 \quad (44)$$

- A degenerate band edge of axial dispersion relation

$$\frac{\partial\omega}{\partial k_z} = 0, \quad \frac{\partial^2\omega}{\partial k_z^2} = 0, \quad \frac{\partial^3\omega}{\partial k_z^3} = 0, \quad \frac{\partial^4\omega}{\partial k_z^4} \neq 0 \quad (45)$$

The above definitions are analogous to those in (9), (12), and (16), related to the case of normal propagation. We still can refer to the $k - \omega$ diagrams in Fig. 1, where the quantity k is now understood as the normal component k_z of the Bloch wavenumber at fixed \vec{k}_\perp .

In order to further establish a close analogy between the cases of normal and oblique propagation, let us introduce some standard procedure commonly used in electrodynamics of layered media. In the case of oblique propagation, the time-harmonic electric and magnetic fields $\vec{E}(x, y, z)$ and $\vec{H}(x, y, z)$ depend on all three Cartesian coordinates, both inside (at $z > 0$) and outside (at $z < 0$) the periodic medium. Given the boundary conditions (41), the field dependence on the transverse coordinates x and y can be accounted for by the following substitution in the time-harmonic Maxwell equations

$$\vec{E}(\vec{r}) = e^{i(k_x x + k_y y)} \vec{\mathcal{E}}(z), \quad \vec{H}(\vec{r}) = e^{i(k_x x + k_y y)} \vec{\mathcal{H}}(z). \quad (46)$$

The next step is a separation of the transverse components of $\vec{\mathcal{E}}(z)$ and $\vec{\mathcal{H}}(z)$ into a close system of four linear differential equations

$$\partial_z \Psi(z) = i \frac{\omega}{c} M(z) \Psi(z), \quad (47)$$

where $\Psi(z)$ is a vector-column

$$\Psi(z) = \begin{bmatrix} \mathcal{E}_x(z) \\ \mathcal{E}_y(z) \\ \mathcal{H}_x(z) \\ \mathcal{H}_y(z) \end{bmatrix} \quad (48)$$

similar to that in (1). An explicit expression for the matrix $M(z)$ can be found, for example, in Ref. [13], along with the detailed discussion of its analytical properties.

In the case of oblique incidence, the 4×4 matrix $M(z)$ in the time-harmonic Maxwell equations (47) depends not only on physical parameters of the periodic structure, but also on the tangential components $\vec{k}_\perp = (k_x, k_y)$ of the wave vector. In the particular case of normal propagation, the symmetry of the 4×4 matrix $M(z)$ in (47) increases so that it may become incompatible with the existence of a stationary inflection point (12) and/or a degenerate band edge (16). This is why the axial frozen

mode regime at oblique incidence can occur in some periodic structures which are too simple to support the normal frozen mode regime. Examples such structures are presented in Figs. 3 and 4.

All basic features of axially frozen mode regime at oblique incidence are virtually the same as in the case of normal propagation. In particular, all the formulae of the previous section describing the structure and composition of the transmitted field $\Psi_T(z)$ remain unchanged. This close similarity holds both for the frozen mode regime at a stationary inflection point (44) and at a degenerate band edge (45). In either case, Figs. 7 through 10 give an adequate idea of the frozen mode structure. Still, there is one essential difference. Namely, in the case of axially frozen mode we have to remember that the tangential component of the group velocity is not zero, even if the normal component (40) vanishes. This means that the axially frozen mode is in fact an abnormal grazing mode with purely tangential energy flux, greatly enhanced amplitude, and very unusual profile. In the next subsection we elaborate on this point.

3.2. Axially frozen mode as an abnormal grazing wave

3.2.1. Stationary inflection point of axial dispersion relation Let us start with the case (12) of stationary inflection point. In the vicinity of ω_0 , the transmitted wave $\Psi_T(z)$ is a superposition (22) of propagating and evanescent Bloch eigenmodes. According to (25), both contributions to $\Psi_T(z)$ have huge and nearly equal and opposite values near the photonic crystal boundary, so that $\Psi_T(0)$ is small enough to satisfy the boundary condition (3). As the distance z from the slab boundary increases, the evanescent component $\Psi_{ev}(z)$ decays exponentially, while the amplitude of the propagating component $\Psi_{pr}(z)$ remains constant and very large. As the result, the field amplitude reaches its huge saturation value at a certain distance (28) from the slab boundary, as illustrated in Fig. 7.

Let us now introduce a unit vector \vec{n} parallel to the direction of incident wave propagation

$$n_x = k_x c / \omega, \quad n_y = k_y c / \omega, \quad n_z = \sqrt{1 - (n_x^2 + n_y^2)}, \quad (49)$$

and let \vec{n}_0 and ω_0 be the direction of incidence and the frequency corresponding to a stationary inflection point (44) of the axial dispersion relation. When the frequency ω tends to its critical value ω_0 at fixed direction of incidence \vec{n}_0 , the saturation value Ψ_{pr} of the transmitted wave amplitude diverges as $|\omega - \omega_0|^{-1/3}$, according to (25). This behavior is illustrated in Fig. 6. Conversely, when the direction of incidence \vec{n} tends to its critical value \vec{n}_0 at fixed frequency ω_0 , the respective saturation value Ψ_{pr} of the transmitted wave amplitude diverges as $|\vec{n} - \vec{n}_0|^{-1/3}$.

Consider now the frozen mode regime at oblique incidence in terms of refraction of the incident plane wave at the photonic crystal boundary. In Fig. 13 we show a wide monochromatic beam of frequency ω incident on the surface of the semi-infinite photonic crystal. The refraction angle θ_T is determined by the ratio of the normal and tangential components of the group velocity

$$\frac{\pi}{2} - \theta_T = \arctan \frac{u_z}{u_\perp}. \quad (50)$$

The direction of incidence $\vec{n}_0 \parallel \vec{S}_I$ in Fig. 13 is chosen so that the condition (44) of the frozen mode regime is satisfied at $\omega = \omega_0$. As frequency ω tends to ω_0 from either

direction, the normal component u_z of the transmitted wave group velocity vanishes, while the tangential component \vec{u}_\perp remains finite

$$u_z \sim |\omega - \omega_0|^{2/3} \rightarrow 0, \quad \vec{u}_\perp \rightarrow \vec{u}_0 \quad \text{as } \omega \rightarrow \omega_0. \quad (51)$$

This relation together with (50) yield

$$\frac{\pi}{2} - \theta_T \propto |\omega - \omega_0|^{2/3} \rightarrow 0 \quad \text{as } \omega \rightarrow \omega_0. \quad (52)$$

Evidently, in the vicinity of the frozen mode frequency, the transmitted (refracted) propagating mode can be viewed as a grazing mode, because its group velocity becomes parallel to the surface.

The most important and unique feature of this abnormal grazing mode directly relates to the fact that the transmittance of the photonic crystal remains finite even at $\omega = \omega_0$. Indeed, let A_I and A_T be the cross-section areas of the incident and transmitted (refracted) beams in Fig. 13, respectively. Obviously,

$$\frac{A_T}{A_I} = \frac{\cos \theta_T}{\cos \theta_I} \quad (53)$$

Let us also introduce the quantities

$$U_I = A_I S_I, \quad U_T = A_T S_T, \quad (54)$$

where S_I and S_T are the energy fluxes of the incident and transmitted waves. U_I and U_T are the total power transmitted by the incident and refracted beams, respectively. The expressions (53) and (54) imply that

$$\frac{U_T}{U_I} = \frac{S_T \cos \theta_T}{S_I \cos \theta_I} = \frac{(S_T)_z}{(S_I)_z} = \tau \quad (55)$$

which is nothing more than a manifestation of the energy conservation. Equation (55) together with (52) yield

$$S_T = \tau S_I \frac{\cos \theta_I}{\cos \theta_T} \propto |\omega - \omega_0|^{-2/3} \rightarrow \infty \quad \text{as } \omega \rightarrow \omega_0. \quad (56)$$

where we have taken into account that $\tau \cos \theta_I$ is of the order of unity, as $\omega \rightarrow \omega_0$.

The expressions (52 – 56) show that in the vicinity of the frozen mode regime, the transmitted beam is a grazing mode with very large intensity S_T and sharply reduce cross-section area A_T , compared to those of the incident beam. By contrast, in the vicinity of the photonic band edge the transmittance τ of the semi-infinite slab vanishes along with the normal component of the energy flux \vec{S}_T of the transmitted (refracted) wave.

The above qualitative analysis is only valid on the scales larger than the characteristic length Z in (28). The value Z defines the distance from photonic crystal surface, where the evanescent contribution to the transmitted wave is still significant. The latter restriction implies that the width of both the incident and the refracted beams must be much larger than Z . Otherwise, the transmitted wave cannot be treated as a beam, and the expressions (52 – 56) do not apply.

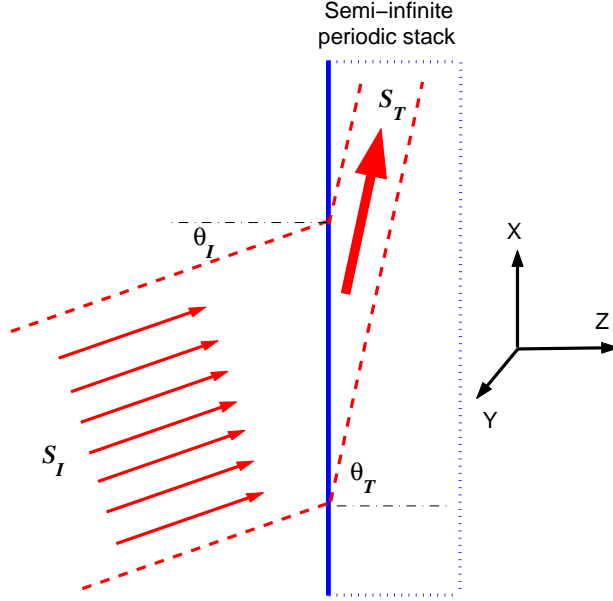


Figure 13. Incident and transmitted (refracted) waves in the vicinity of the axial frozen mode regime. The reflected wave is not shown. θ_I and θ_T are the incidence and refraction angles, S_I and S_T are the energy density fluxes of the incident and transmitted waves. Both the energy density and the energy density flux in the transmitted wave are much larger than the respective values in the incident wave. However, the total power transmitted by the refracted wave is smaller by factor τ , due to much smaller cross-section area of the nearly grazing transmitted wave.

3.2.2. Degenerate band edge of axial dispersion relation Below the degenerate band edge frequency ω_d in (45), the transmitted wave $\Psi_T(z)$ is a superposition (22) of propagating and evanescent Bloch eigenmodes. According to (30), both contributions to $\Psi_T(z)$ have very large and nearly equal and opposite values near the photonic crystal boundary at $z = 0$, so that $\Psi_T(0)$ is small enough to satisfy the boundary condition (3). As the distance z from the slab boundary increases, the evanescent component $\Psi_{ev}(z)$ decays exponentially, while the amplitude of the propagating component $\Psi_{pr}(z)$ remains constant and very large. As the result, the field amplitude reaches its huge saturation value at a certain distance from the slab boundary, as illustrated in Fig. 7. At first sight, this scenario is similar to the case of oblique frozen mode regime at stationary inflection point of the axial dispersion relation. But there is an important difference. As the frequency ω tends to its critical value ω_d , the photonic crystal reflectivity approaches unity, implying total reflection of the incident radiation. In this respect, the situation below an axial degenerate band edge is reminiscent of the classical phenomenon of total internal reflection. The difference, though, is that the transmitted wave profile $\Psi_T(z)$ is the same as in the previously discussed case of stationary inflection point of the axial dispersion relation. It implies that just below a degenerate band edge frequency of axial dispersion relation, the transmitted wave can be classified as an abnormal grazing mode with large diverging amplitude and large tangential component of the energy flux. The typical profile of such a grazing mode

at $\omega \lesssim \omega_d$ is shown in Figs. 8(a) and 10(a – b).

If the incident wave frequency lies slightly above ω_d (in the band gap), the transmitted wave $\Psi_T(z)$ is a superposition (21) of two evanescent Bloch eigenmodes. The energy flux in the abnormal grazing mode now is strictly parallel to the surface, regardless of small variations in frequency and/or direction of propagation of the incident wave. This is a direct consequence of the total reflectivity of photonic crystals at band gap frequencies. The grazing mode profile in this case is shown in Figs. 9(a) and 10(d – f). As the frequency ω approaches its critical value ω_d , the amplitude and the thickness of the grazing mode diverge in accordance with (35) and (33), respectively.

3.2.3. Surface waves in the vicinity of a degenerate band edge of axial dispersion relation So far in this section we have tacitly assumed that

$$k_x^2 + k_y^2 < \omega^2 c^2. \quad (57)$$

The inequality (57) implies that the z component (42) of the wave vector of the incident and reflected waves is real. This is a natural assumption when considering the problem of a plane wave incident on a semi-infinite photonic crystal.

Consider now the opposite case where

$$k_x^2 + k_y^2 > \omega^2 c^2. \quad (58)$$

In this situation, there is no plane propagating waves in vacuum matching the boundary conditions (41) at the surface. Still, if the frequency ω lies above the band edge of the axial dispersion relation (in the band gap), a superposition (21) of two forward evanescent eigenmodes with $k_z'' > 0$ can produce a surface wave exponentially decaying with the distance z from the boundary in either direction. As the frequency ω approaches the degenerate band edge value ω_d for a given \vec{k}_\perp , the surface wave profile can become similar to that of an abnormal grazing mode at $\omega \gtrsim \omega_d$, shown in Figs. 9(a) and 10(d – f). Although formally, it is still a surface wave, its profile now is highly unusual for a surface wave. Namely, the field amplitude in the periodic medium sharply increases with the distance z from the surface, reaches its maximum at a distance Z defined in (33), and only after that it begins a slow decay.

4. Conclusion

In this paper we outlined several different manifestations of the frozen mode regime in photonic crystals. Although all our numerical examples relate to periodic layered structures, in fact, the frozen mode regime is more like a universal wave phenomenon. Indeed, we can talk about different kinds of wave excitations in low-loss periodic media. But as soon as the respective Bloch dispersion relation displays a singularity like a stationary inflection point (44) or a degenerate band edge (45), we have every reason to expect a very similar behavior involving the frozen mode regime. In other words, the possibility of the frozen mode regime is determined by some fundamental spectral properties of the periodic structure. If a periodic array is relatively simple, for instance, a stratified medium with one dimensional periodicity, its frequency spectrum may prove to be too simple to support the proper spectral singularity. The more complex the periodic structure is, the more likely it will be capable of supporting such

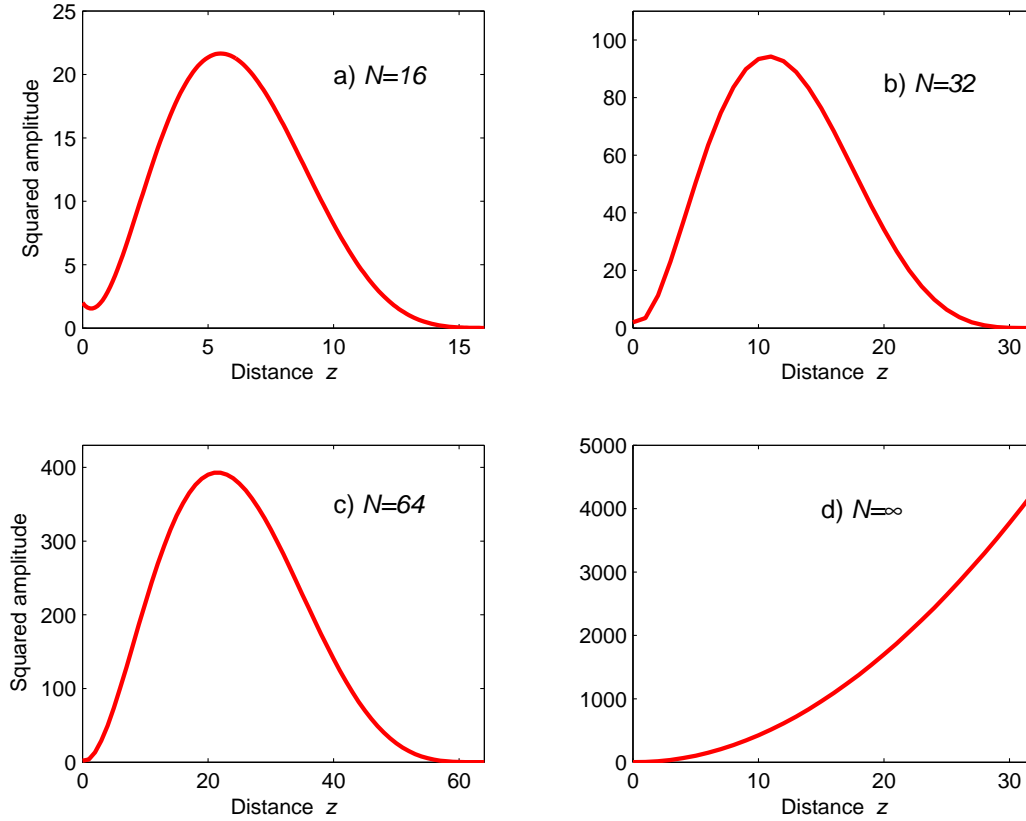


Figure 14. Smoothed profile of the frozen mode in periodic layered structures composed of different number N of unit cells L in Fig. 2. The frequency is equal to that of degenerate band edge. The initial rate of growth of the frozen mode amplitude is independent of N and described by (34). The limiting case (d) of the semi-infinite structure is also shown in Fig. 10(c). In all cases, the incident wave has the same polarization and unity amplitude.

a phenomenon. For instance, in the case of layered arrays we need birefringent layers and, sometimes, at least three layers in a unit cell.

Another important question is how robust the frozen mode regime is. For instance, what happens if we introduce a small absorption or structural imperfections? Of course, these factors suppress the frozen mode amplitude. But in this respect, the frozen mode regime is no different from any other coherent or resonance effects in periodic structures. This problem can be solved at any particular frequency range by appropriate choice of the constitutive materials.

Another fundamental restriction relates to the size of the periodic structure. In this paper we assumed that the periodic array occupies the entire half-space $z \geq 0$. A good insight on what happens to the frozen mode in a finite periodic array is given by Fig. 14. These graphs prove that the frozen mode regime in a finite periodic array can be as robust as that in an imaginary semi-infinite structure. The optimal number of layers depends on such factors as the absorption characteristics of the constitutive materials, the geometrical imperfections of the periodic array, the desired degree of

field enhancement in the frozen mode, etc. On the other hand, in finite (bounded) photonic crystals, some new resonance phenomena can arise, such as transmission band edge resonances [2, 3, 14]. These effects, though, occur at slightly different frequencies and are qualitatively different from the frozen mode regime.

Acknowledgment and Disclaimer: Effort of A. Figotin and I. Vitebskiy is sponsored by the Air Force Office of Scientific Research, Air Force Materials Command, USAF, under grant number FA9550-04-1-0359.

- [1] J. Joannopoulos, R. Meade, and J. Winn. *Photonic Crystals*. (Princeton University Press, 1995).
- [2] Pochi Yeh. "Optical Waves in Layered Media", (Wiley, New York, 1988).
- [3] Weng Cho Chew. "Waves and Fields in Inhomogeneous Media", (Van Nostrand Reinhold, New York, 1990).
- [4] L. Brillouin. *Wave Propagation and Group Velocity*. (Academic, New York, 1960).
- [5] M. Notomi. *Theory of light propagation in strongly modulated photonic crystals: Refractionlike behavior in the vicinity of the photonic band gap*. Phys. Rev. **B62**, 10696 (2000)
- [6] L. D. Landau, E. M. Lifshitz, L. P. Pitaevskii. *Electrodynamics of continuous media*. (Pergamon, N.Y. 1984).
- [7] A. Yariv and Pochi Yeh. *Optical Waves in Crystals*. ("A Wiley-Interscience publication", 1984).
- [8] A. Figotin, and I. Vitebskiy. *Nonreciprocal magnetic photonic crystals*. Phys. Rev. **E63**, 066609 (2001).
- [9] A. Figotin, and I. Vitebskiy. *Electromagnetic unidirectionality in magnetic photonic crystals*. Phys. Rev. **B67**, 165210 (2003).
- [10] A. Figotin, and I. Vitebskiy. *Oblique frozen modes in layered media*. Phys. Rev. **E68**, 036609 (2003).
- [11] J. Ballato, A. Ballato, A. Figotin, and I. Vitebskiy. *Frozen light in periodic stacks of anisotropic layers*. Phys. Rev. **E71**, (2005).
- [12] A. Figotin and I. Vitebskiy. *Electromagnetic unidirectionality and frozen modes in magnetic photonic crystals*. JMMM, **300**, 117 (2006).
- [13] A. Figotin and I. Vitebskiy. *Slow light in photonic crystals (Topical Review)*. Waves in Random Media, Vol. 16, No. 3, 293–382 (2006).
- [14] A. Figotin and I. Vitebskiy. *Gigantic transmission band-edge resonance in periodic stacks of anisotropic layers*. Phys. Rev. **E72**, 036619, (2005).